Determination of austenite vs. -ferrite in steel by neutron and x-ray diffraction

Als-Nielsen, Jens Aage; Clausen, K.N.

Publication date:
1984

Document Version
Publisher's PDF, also known as Version of record

Citation (APA):
Als-Nielsen, J. A., & Clausen, K. N. (1984). Determination of austenite vs. -ferrite in steel by neutron and x-ray diffraction. (Risø-M; No. 2439).

DK8400126

RISØ-M-2430

RISØ

RISØ-M-2430

Determination of Austenite vs. α-ferrite in Steel by Neutron and X-ray Diffraction

J. Als-Nielsen, K. Clausen

Risø National Laboratory, DK-4000 Roskilde, Denmark
June 1984

RISØ-M-2439

DETERMINATION OF AUSTENITE vs. α-FERRITE IN STEEL BY NEUTRON AND X-RAY DIFFRACTION

J. Als-Nielsen and K. Clausen
Physics Department

Abstract. Neutron and X-ray diffraction studies for determining the relative content of fcc (austenite) and bcc (α-ferrite) phases in steel samples are reported. In addition to determine the relative content of phases the diffraction method also provides information about the strain fields in the sample by the concomitant broadening of diffraction peaks. Neutron diffraction has the advantage that large sample volumes (several cc) are probed, and the effect of texture can thus be eliminated. X-ray diffraction patterns can be registered in a short time thus allowing kinetic studies of phase changes during heat treatment or mechanical treatment. In addition it is possible to probe different surface thickness by utilizing different X-ray wavelengths. Measurements of this type can be carried out on a commercial contract basis in the Solid State Physics Division at Risø National Laboratory.

INIS descriptors: AUSTENITE; NEUTRON DIFFRACTION; QUALITY CONTROL; STAINLESS STEELS; X-RAY DIFFRACTION

UDC 539.26 (669.112.227.1 + 669.112.228.1)

June 1984
Risø National Laboratory, DK-4000 Roskilde, Denmark

ISBN 87-550-1020-2
ISSN 0418-6435

Risø Repro 1984

CONTENTS Page

1. INTRODUCTION 5

2. DIFFRACTION METHODS 5

3. EXPERIMENTAL SET UP 7
   3.1. Neutron Diffraction 7
   3.2. X-Ray Diffraction 8
   3.3. Samples 8

4. RESULTS 9
   4.1. NBS Standard Sample 9
   4.2. Stainless Steel Sample 10

5. FIGURES 11

1. INTRODUCTION

Pure iron crystalizes from the melt of 1540°C in the bcc phase (δ). At a lower temperature 1400°C, a crystallographic transformation to the closed-packed fcc phase (γ) takes place. By further cooling another transformation to a bcc phase (α) occurs at 910°C. This phase becomes ferromagnetic at the Curie temperature of 768°C.

Steels are alloys of iron with carbon and possibly other 3d-metals as for instance Chromium. The crystallographic phases corresponding to the γ- and α-phases of pure iron are called austenite and α-ferrite, respectively. These phases have different solubility of carbon, and in equilibrium an eutectic transformation at 0.8% carbon content takes place at 724°C, but supercooling of the austenite phase all the way to ambient temperature is certainly possible. Eventually the fcc austenite can change to bcc but since this phase cannot in equilibrium accommodate the eutectic 0.8% carbon content it distorts to a tetragonal body centered structure, martensite, with a larger specific volume than the closed-packed austenite phase. Martensite and austenite have quite different mechanical and corrosion properties giving rise to the broad spectrum of steels. The relative content of austenite, α-ferrite or martensite can be changed by heat treatments like hardening and tempering, and since the cooling rate is faster at the surface than in the bulk the relative content of phases and the associated mechanical properties are generally not homogeneous.

It is important for the manufacturer as well as the customer to asses and know the relative amount of phases for a given type of steel. This can be determined by crystallographic means.

2. DIFFRACTION METHODS

The most common diffraction method utilizes X-rays. However, corpuscular beams of electrons or neutrons with wavelengths in the X-ray range will be diffracted by the same fundamental principles known as Bragg scattering. However, there are important practical differences. X-rays can in addition to scattering undergo absorption, a process which depends strongly on the X-ray wavelength. Neutrons are absorbed to a much lesser extent and the 1/e absorption length in iron for X-rays and neutrons are shown as function of wavelength in fig. 1. Thus X-rays from a Cu-anode penetrate only a few microns into Fe whereas neutrons penetrate of the order of one centimeter. This has several implications.It is not easy to avoid at least some change in the ratio of crystallographic phases by mechanical treatment, such as e.g. grinding or by etching in a surface layer thickness of the order of microns, i.e. the Cu X-ray penetration depth. Furthermore, to interpret diffraction data one must consider texture of the polycrystalline material, or to be more specific one would like to ensure a proper spherical average of grain orientation within the irradiated part of the samle. Clearly a large penetration depth makes this task easier. On the other hand an systematic study of the diffraction pattern versus X-ray wavelength may be valuable in order to asses the heterogeneity of phase composition alluded to in the introduction. The present study using neutron diffraction yields average composition of the bulk and proper elimination of texture problems is ensured.

We shall now briefly recall the crystallography of fcc (austenite) and bcc (α-ferrite) phases. The Bragg reflections are characterized by so-called Miller indices which simply are the Cartesian coordinates of the normal to the reflecting planes. Thus the (111) reflection is due to planes of Fe atoms perpendicular to the cube-diagonal. Interference effects imply that certain reflections can vanish and these selection rules are different for the fcc and bcc lattices. The intensity of the reflections gives the ratio of the two phases, although not directly. One has for instance to take multiplicity into account. The corner of the unit cell cube is the vertex of 6 cube-edges, 8 cube-diagonals and 12 face-diagonals so for the fcc lattice, where both (111) and (200) are allowed reflections there is an 8:6 better chance to hit a grain in the (111) orientation than one in the (200) orientation. In addition there are some geometrical factors depending on the Bragg angle θ which is related to the monochromatic wavelength λ and the plane spacing d by $\lambda=2d\sin\theta$ (Bragg's law).

Neutrons are, in contrast to X-rays, diffracted from an Fe crystallite by two basic mechanisms: interactions due to nuclear forces and the dipolar magnetic interaction between the magnetic moment of the neutron and the Fe atom in its ferromagnetic state. Since austenite is non-magnetic and α-ferrite is ferromagnetic, the latter scatters neutrons somewhat more than expected from the simple composition ratio. Fortunately, this complication can be safely corrected for. If the magnetic moment of the Fe atoms bisects the scattering angle the magnetic scattering is eliminated; on the other hand, if the magnetic moment of the Fe atom is perpendicular to the scattering plane the magnetic scattering attains its maximal value. Thus by applying a magnetic field in these two directions the intensity due to magnetic scattering can be determined unambiguously. Quantitatively, the nuclear scattering amplitude $b_n=0.96\ 10^{-12}$ cm whereas the effective magnetic scattering amplitude around the (110) reflection assuming a magnetic moment of $2.2\mu_B$ per Fe atom in the α-ferrite phase is $b_m=0.44\ 10^{-12}$ cm. With maximal magnetic scattering the relative contribution to the intensity is thus $(.44/.96)^2$ and for an unmagnetized sample the effect is only $1/3\ (.44/.96)^2 \approx 7\%$.

3. EXPERIMENTAL SET UP

3.1 Neutron Diffraction

We shall here briefly describe the experimental setup so similar future studies can be compared to the present one and the performance of other neutron diffractrometers around the DR 3 reactor can be assessed.

The measurements were carried out at diffractrometer TAS 7 which is situated in the neutron guide hall adjacent to DR 3.

Neutrons from the cold source are totally reflected in a slightly bent guide tube. A monochromatic beam of wavelength 2.39 Å is extracted by (002) Bragg reflection from a 12 cm high pyrolytic graphite crystal, bent to focus the beam to a 2 cm high beam spot at the sample position. Soller collimators with angular divergence of 36′ and 28′ were applied before and after the sample and 35′ between analyzer and detector. In order to reduce background the diffracted beam is Bragg reflected from an analyzer crystal, a flat, pyrolytic graphite crystal in the (002) orientation.

3.2 X-Ray Diffraction

A 10 kW rotating Molybdenum anode was used for generating X-rays. The K_α line was extracted from the beam by Bragg reflection from a bent pyrolytic graphite crystal using the (004) reflection. The monochromatic beam passed an aperture of 0.6 x 2 mm^2 in front of the sample slab which was orientated in reflection geometry. The scattered beam was detected in a horizontal position sensitive detector, PSD, with a sensitive area of about 40 mm wide and 10 mm high. A flight tube between the sample and the PSD was inserted to reduce background radiation. Furthermore a 0.5 mm thick Aluminium foil was inserted in the scattered beam to eliminate the fluorescent iron X-ray radiation. The entire diffraction patterns as those shown in fig. 3 and 5 can be obtained within a few minutes. The X-ray set up has thus the potential of observing the kinetics of phase changes during heat treatments although such studies are not reported here.

3.3 Samples

Two samples were investigated. The first sample is a standard sample from National Bureau of Standards, 21 mm diam. and 2.5

mm thick, containing nominally 4.6% austenite.

This sample was assumed to be texture free, and the disc was bisecting the scattering angle. This sample could be situated in a permanent magnet yoke with a sample gap of 25 mm and a magnetic field of about 1 kGauss. The yoke could be mounted on the sample table in two orientations with the magnetic field vertical or horizontal bisecting the scattering angle.

The second sample contained nominally 0.2% α-ferrite in an austenite matrix. It was composed by a stack of ten 25 mm x 25 mm squares cut out of a 1.5 mm thick sheet with angular increment of 10° of each square relative to the rolling direction. This sample was constantly rotated around a vertical axis at 60 rpm during the measurements. The stacking and the rotation presumably eliminate texture effects in the data. This sample could also be placed in the magnetic yoke but rotation is then prohibited as the yoke will intercept the incoming and scattered beams.

All measurements were carried out at room temperature.

4. RESULTS

4.1 NBS Standard Sample

Fig. 2 shows a scan through the (111) peak of the fcc austenite phase around 3.03 $Å^{-1}$, and the (110) peak of the bcc α-ferrite phase around 3.10 $Å^{-1}$ using neutrons. Similar data using Mo K_α X-rays (wavelength 0.7107 Å) is shown in fig. 3 utilizing a position sensitive detector to register all points simultaneously. The low background level in fig. 3 is accomplished by absorbing the Fe fluorescense radiation (wavelength 1.937 Å) in a 0.5 mm thick Aluminium foil.

The wing on the small wavevector side of the strong (110) peak contributes to the intensity at the position of the small peak. This contribution is determined by assuming that the peak is symmetric, i.e. by symmeterizing around the peak position. Taking the multiplicity into account (and correcting for the magnetic contribution in the neutron case) we find an austenite content of 4.7±0.5% from X-ray data and 4.2±0.5% from neutron data to be compared with a nominal value of 4.6±0.2% for the NBS sample.

4.2 Stainless Steel Sample

Neutron data of the SS sample is shown in fig. 4. Assuming a sloping background as shown and estimating the high wavevector wing of the strong peak by the symmeterizing procedure outlined above we obtain a small α-ferrite peak around Q=3.0985 $Å^{-1}$ corresponding to 0.8% content of this phase. The estimated systematic error is 0.5%. It should be noted that the width of the austenite peak (.040 $Å^{-1}$) and of the α-ferrite peak (.06 $Å^{-1}$) are significantly larger than the resolution width (0.030 $Å^{-1}$) as observed in fig. 2. The peak broadening in the SS sample is presumably due to the strain fields in the stainless steel and the intrinsic widths may be converted to stress fields. The quoted α-ferrite content is bases upon integrated intensities, not peak intensities.

X-ray data of the SS sample is shown in fig. 5. Again a small α-ferrite signal is evident. The peak widths of austenite phase and α-phase are 0.025 $Å^{-1}$ and 0.043 $Å^{-1}$ respectively. From the ratio of integrated intensities we find an α-ferrite content of 2.0% with an estimated error of ±0.5%.

Both neutron and X-ray results show that the α-ferrite content in the SS sample is quite small, of the order of 1% and both methods indicate a peak broadening at least of the α-ferrite phase presumably due to strain fields. It should be emphasized that the X-ray results derive from one single arbitrary volume part of about 0.1 mm^3 whereas the neutron data represents an avarage of the total sample volume of about 10^4 mm^3.

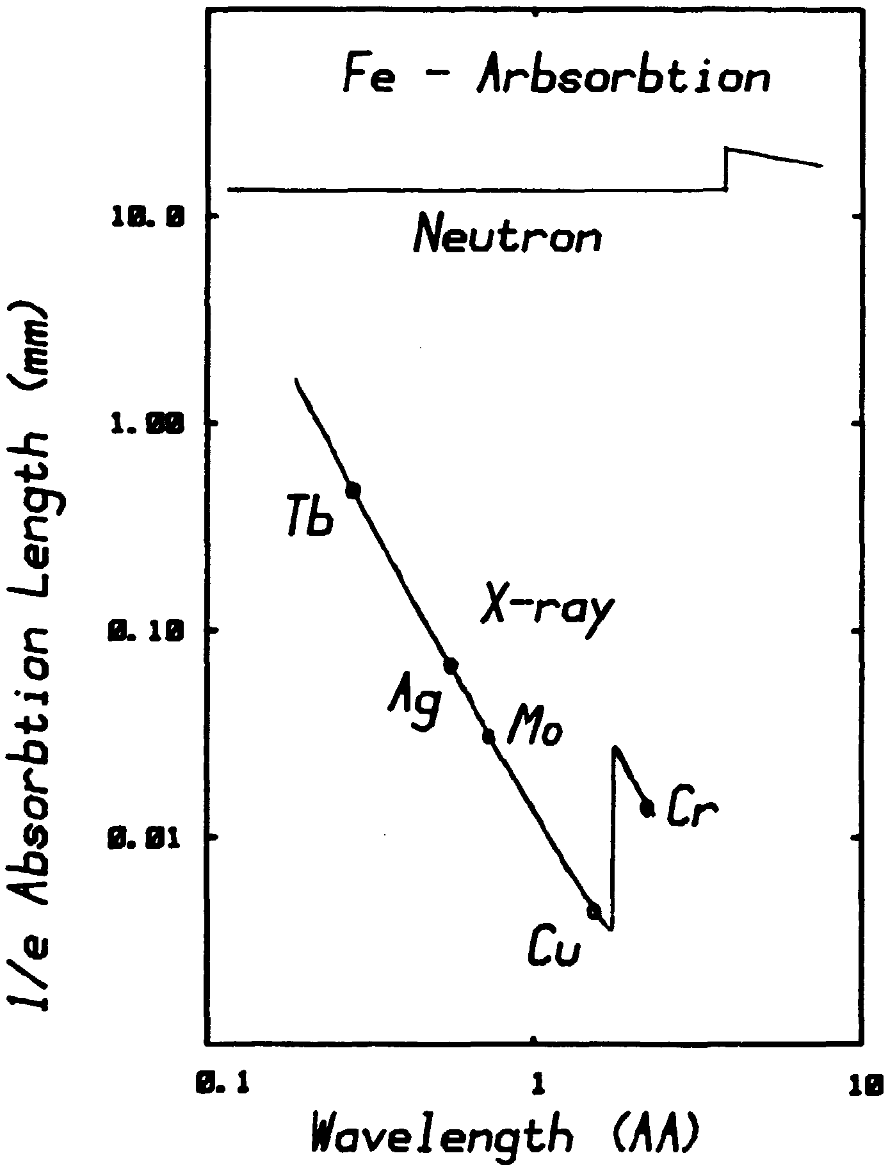

Fig. 1

Wavelength dependence of the 1/e absorbtion length in Fe for X-rays and neutrons. The characteristic K_α-radiation from selected anode materials are marked on the X-ray absorption curve.

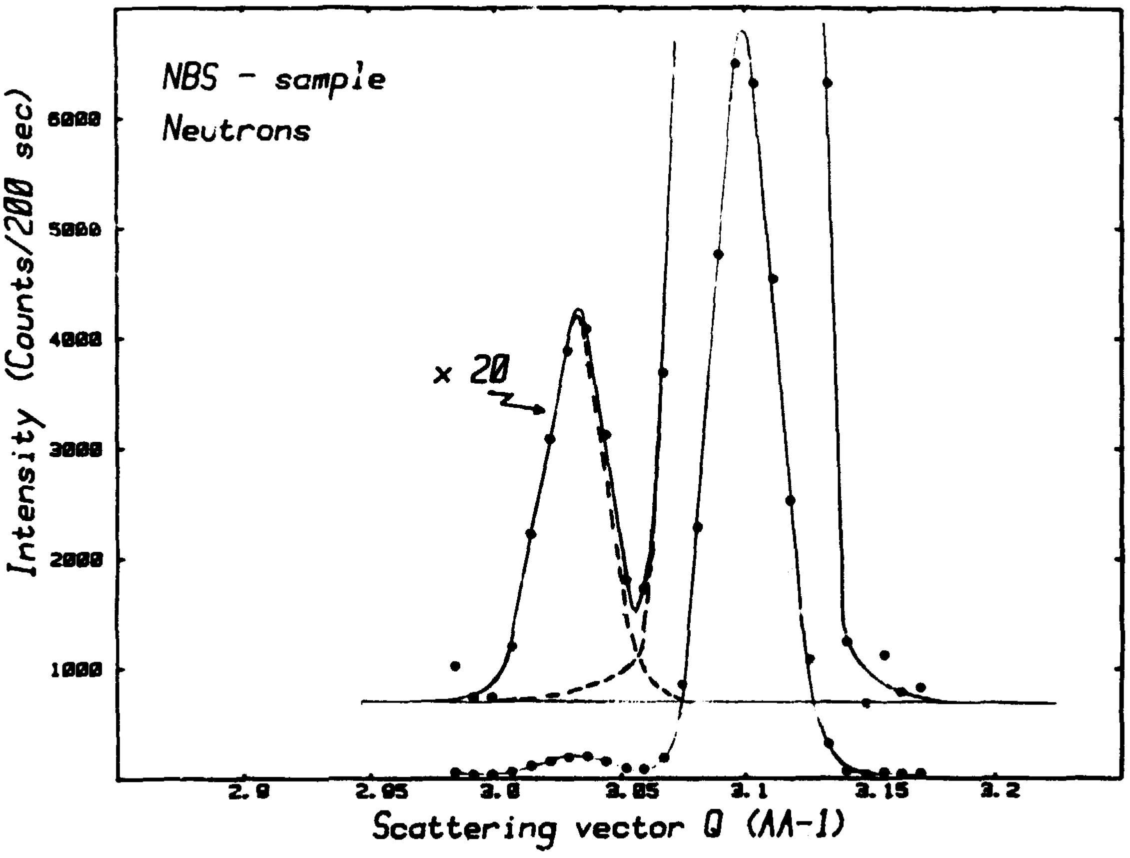

Fig. 2

Diffraction pattern for the NBS Standard sample as observed with neutrons on TAS 7 (Reactor power 10MW). The peak at 3.03 A^{-1} is the (111) reflection from the fcc austenite phase, and the peak at 3.10 A^{-1} is the (110) reflection from the bcc α-ferrite phase. On the 20 times expanded scale we have indicated the background level, the total signal (solid line) and the contributions from the two components (broken line) in the range of overlap between the two peaks.

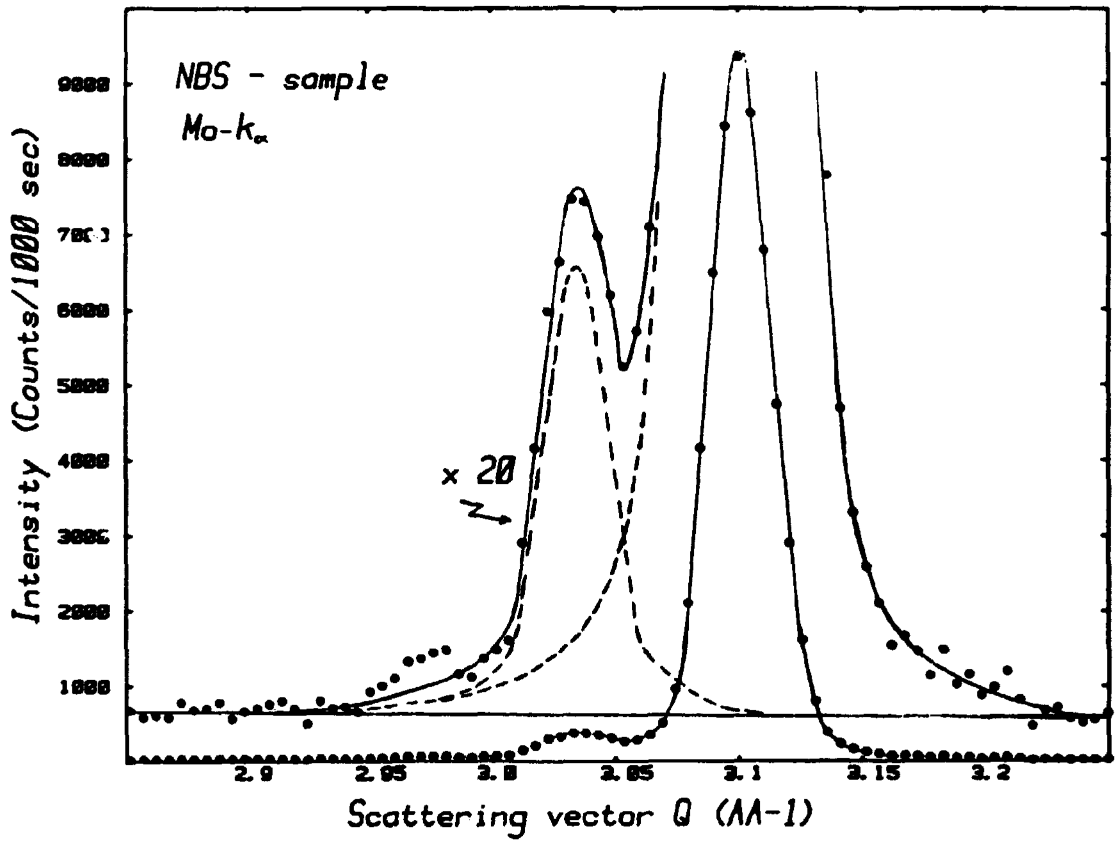

Fig. 3

Diffraction pattern for the NBS standard sample as observed with a position sensitive detector on the rotating anode X-ray source (Mo K_α, 40 kV and 100 mA), for further explanation of the curve see caption for fig. 2.

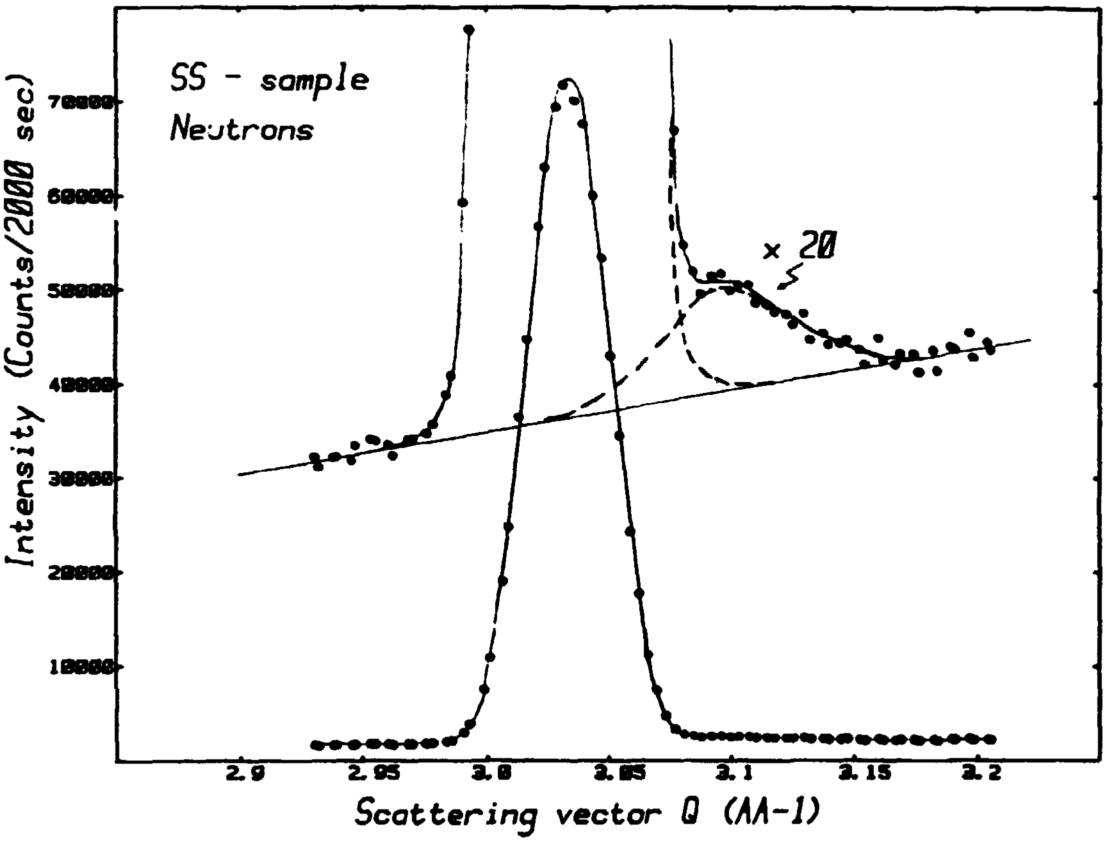

Fig. 4.

Diffraction pattern for the SS, Stainless Steel sample as observed with neutrons on TAS 7 (Reactor power 5MW). See caption for fig. 2

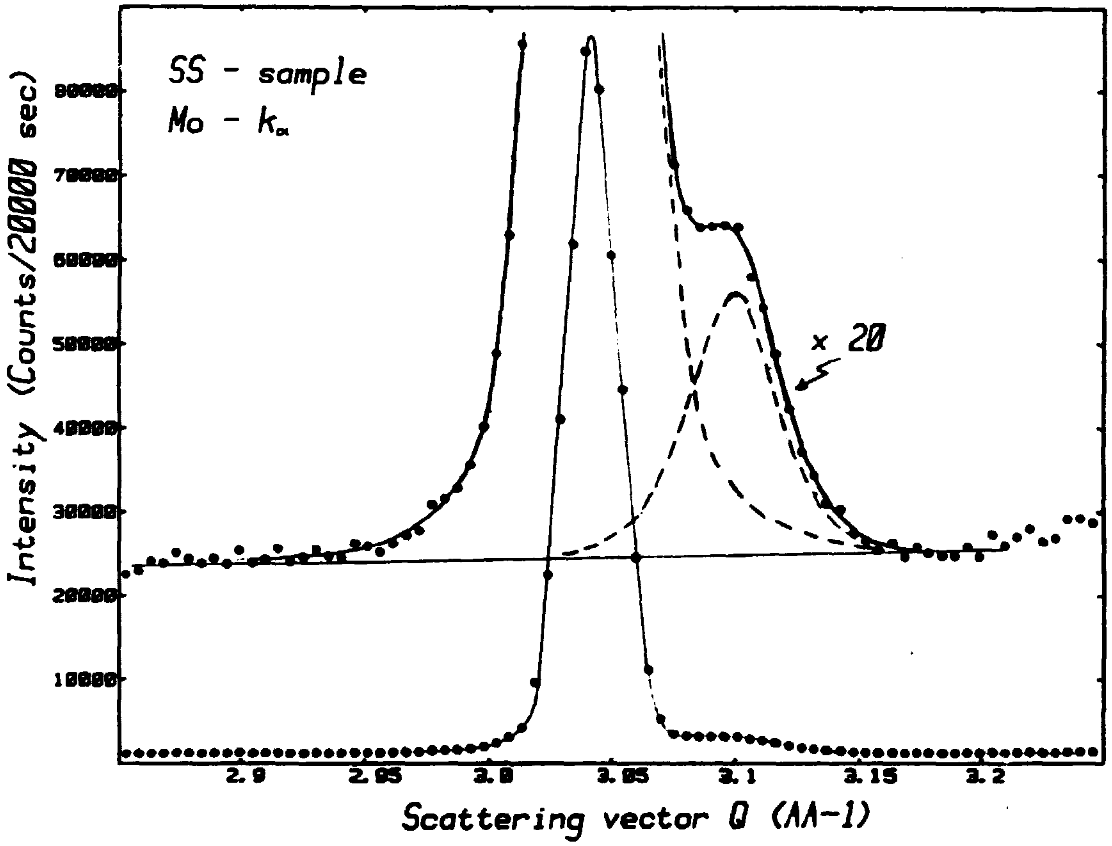

Fig. 5

Diffraction pattern for the SS, Stainless Steel sample as observed with a position sensitive detector on the rotating anode X-ray source (Mo K_α, 40 kV and 100 mA). See caption for fig. 2.

Risø National Laboratory **Risø - M - 2439**

Risø - M - 2439

Title and author(s)

DETERMINATION OF AUSTENITE vs. α-FERRITE IN STEEL BY NEUTRON AND X-RAY DIFFRACTION

J.Als-Nielsen and K.Clausen
Physics Department

Date 6.7.1984

Department or group
Physics

Group's own registration number(s)

15 pages + tables + 5 illustrations

Abstract

Neutron and X-ray diffraction studies for determining the relative content of fcc (austenite) and bcc (α-ferrite) phases in steel samples are reported. In addition to determine the relative content of phases the diffraction method also provides information about the strain fields in the sample by the concomitant broadening of diffraction peaks. Neutron diffraction has the advantage that large sample volumes (several cc) are probed, and the effect of texture can thus be eliminated. X-ray diffraction patterns can be registered in a short time thus allowing kinetic studies of phase changes during heat treatment or mechanical treatment. In addition it is possible to probe different surface thickness by utilizing different X-ray wavelengths. Measurements of this type can be carried out on a commercial contract basis in the Solid State Physics Division at Risø National Laboratory.

Copies to

Available on request from Risø Library, Risø National
Laboratory (Risø Bibliotek), Forsøgsanlæg Risø),
DK-4000 Roskilde, Denmark
Telephone: (03) 37 12 12, ext. 2262. Telex: 43116

Available on request from.
Risø Library,
Risø National Laboratory, P.O. Box 49,
DK-4000 Roskilde, Denmark
Phone (02) 371212 ext. 2262

ISBN 87-550-1020-2
ISSN 0418-6435